



# Agile Detection of Chemical Warfare Agents by Machine Vision: a Supramolecular Approach

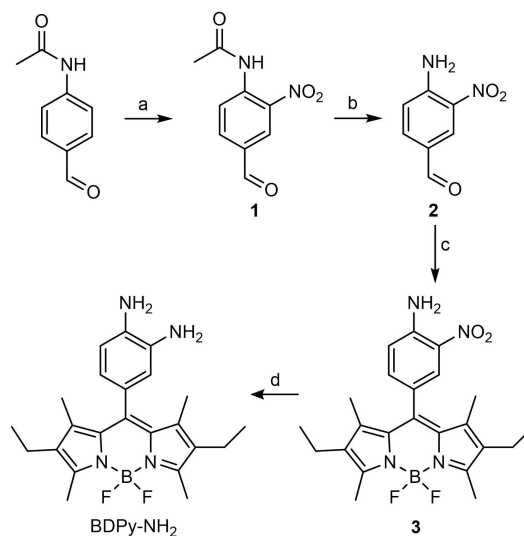
Nunzio Tuccitto,<sup>[a, b]</sup> Gaetano Catania,<sup>[a]</sup> Andrea Pappalardo,<sup>[a, c]</sup> and Giuseppe Trusso Sfrazzetto<sup>\*[a, c]</sup>

**Abstract:** The supramolecular detection by image analysis of a simulant chemical warfare agent on a solid device containing a selective molecular sensor based on a BODIPY scaffold is reported. The recognition properties were investigated in solution, demonstrating high affinity ( $\log K 6.60$ ) and sensitivity (LOD 10 ppt). A test strip also confirmed the sensing properties in gas phase. Image analysis of the solid device allows quantitative information about the simulant to be obtained, recovering the sensor almost 5 times and thus confirming the goal of the supramolecular approach.

Chemical warfare agents (CWAs) are one of the most dangerous types of chemical weapon due to their ability to inhibit acetylcholinesterase (AChE), leading to a cholinergic crisis.<sup>[1]</sup> CWAs, which are divided into 3 different series (G-, V- and A-type),<sup>[2]</sup> were first synthesized in the early decades of the 1900s, but they still represent a serious and concrete risk, due to recent events in Germany,<sup>[3]</sup> the UK,<sup>[4]</sup> Malaysia,<sup>[5]</sup> Syria,<sup>[6]</sup> and Japan.<sup>[7]</sup> For these reasons, today a fast and prompt detection of these compounds is essential to prevent terrorist attacks. Detection methods based on instrumental techniques, such as HPLC or GC-MS, are very sensitive and selective. However, they are expensive and require qualified persons. In contrast, molecular sensing, exploiting molecular interactions between the sensor and the analyte, is easier and faster due to the

possibility to monitor the presence of the analyte by the change in specific characteristics of the sensor (e.g., luminescence, color, conductivity).<sup>[8]</sup> In this context, molecular sensing can be divided into two different approaches: i) a “covalent approach”, in which a covalent reaction occurs between sensor and analyte, leading to the formation of a new compound,<sup>[9]</sup> ii) and the “supramolecular approach” based on the formation of non-covalent interactions between sensor and analyte.<sup>[10–16]</sup> The covalent sensing suffers of some limitations, such as the nonspecific reaction with the analyte leading to false-positive responses and the impossibility to reuse the sensor. On the other hand, supramolecular approach allows to recover the sensor,<sup>[17,18]</sup> and leads to high selectivity for the targeted analyte.<sup>[19–25]</sup> Research activities with CWAs are often not permitted for security reasons, thus less-toxic compounds (simulants) are used for these purposes. In this context, dimethylmethylphosphonate (DMMP) is the most widely used simulant for G-type CWAs.<sup>[26,27]</sup>

Here, the synthesis and the sensing properties of a new DMMP fluorescent sensor (BDPy-NH<sub>2</sub>, Scheme 1) are reported. In particular, we were able to detect DMMP with high efficiency, selectivity and with a sensitivity of ppt levels. In addition, the DMMP sensing was performed both in solution and in gas phase, by using a solid prototype containing BDPy-NH<sub>2</sub>. Due to the high emission properties of the BODIPY scaffold, the



**Scheme 1.** Synthesis of BDPy-NH<sub>2</sub>. a) fuming HNO<sub>3</sub>, RT, 93%; b) HCl 2 M, 120 °C, 16 h, 79%; c) kryptopyrrole, TFA, 2,3-dichloro-5,6-dicyano-1,4-benzoquinone (DDQ), Et<sub>3</sub>N, BF<sub>3</sub>O(Et)<sub>2</sub>, CH<sub>2</sub>Cl<sub>2</sub>, RT, 21%; d) H<sub>2</sub>, Pd/C, CH<sub>3</sub>OH, 94%.

[a] Prof. N. Tuccitto, G. Catania, Prof. A. Pappalardo, Dr. G. Trusso Sfrazzetto  
Department of Chemical Sciences, University of Catania  
95125 Catania (Italy)  
E-mail: giuseppe.trusso@unicat.it

[b] Prof. N. Tuccitto  
Laboratory for Molecular Surfaces and Nanotechnology – CSGI  
95125 Catania (Italy)

[c] Prof. A. Pappalardo, Dr. G. Trusso Sfrazzetto  
National Interuniversity Consortium for Materials Science and  
Technology (I.N.S.T.M.) Research Unit of Catania  
95125 Catania (Italy)

Supporting information for this article is available on the WWW under  
<https://doi.org/10.1002/chem.202102094>

Part of a Special Collection on Noncovalent Interactions.

© 2021 The Authors. Chemistry - A European Journal published by Wiley-VCH GmbH. This is an open access article under the terms of the Creative Commons Attribution Non-Commercial NoDerivs License, which permits use and distribution in any medium, provided the original work is properly cited, the use is non-commercial and no modifications or adaptations are made.

presence of DMMP vapors can be monitored by using a simple smartphone, and a quantification of DMMP vapors can be obtained by image straightforward processing.

BDPy-NH<sub>2</sub> was designed for an easy optical detection of NAs. For this reason, we introduced a BODIPY scaffold as chromophore, and an ortho-diamine aryl moiety, to recognize DMMP via hydrogen bonds.<sup>[20]</sup>

Synthesis was performed by a modified literature protocol: starting from 4-acetamidobenzaldehyde, which after reaction with HNO<sub>3</sub> leads to 3-NO<sub>2</sub>-4-acetamidobenzaldehyde **1**. Deprotection of the amino group was performed by using HCl, obtaining the 3-NO<sub>2</sub>-4-aminobenzaldehyde **2**, which, in the presence of kryptopyrrole, TFA in catalytic amount, DDQ and BF<sub>3</sub>(OEt)<sub>2</sub>, affords the nitro-amino-BODIPY **3**. The reduction of the -NO<sub>2</sub> group with H<sub>2</sub>/Pd leads to the final sensor BDPy-NH<sub>2</sub> (see details in the Supporting Information).<sup>[28,29]</sup> UV-Vis spectrum of BDPy-NH<sub>2</sub> in CHCl<sub>3</sub> shows two main bands, centered at 390

( $\epsilon=2085$ ) and 530 nm ( $\epsilon=21300$ ), respectively. After excitation at 500 nm, emission spectrum shows a strong emission band at 538 nm, typical of the BODIPY chromophores (see the Supporting Information).<sup>[30]</sup> Recognition properties in solution were evaluated monitoring this emission band. In particular, Figure 1 shows the emission spectra of BDPy-NH<sub>2</sub> ( $1 \times 10^{-6}$  M in CHCl<sub>3</sub>) after progressive additions of a DMMP solution ( $1 \times 10^{-4}$  M in CHCl<sub>3</sub>), calculating a binding constant value of log 6.60 for the 1:1 sensor/DMMP stoichiometry, supported by the ESI-MS spectrum (see the Supporting Information).

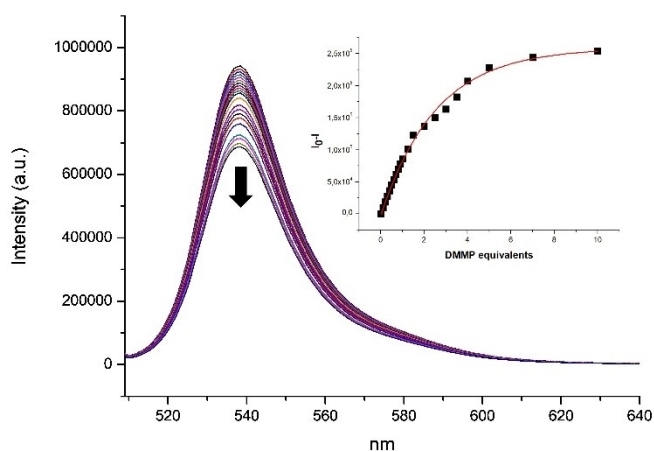
Notably, calculated limit of detection is 9.47 ppt, many orders of magnitude lower than the IDLH (concentration of toxin in air that is immediately dangerous to life and health) values of the common CWAs (2–30 ppb).<sup>[31]</sup>

Selectivity is a crucial parameter for a real sensor. In order to test the selectivity towards DMMP respect to other common interfering analytes, we exposed BDPy-NH<sub>2</sub> to air for 5 minutes, and then the emission spectrum was recorded. As shown in Figure 2, no change of emission intensity was detected, proving the selectivity of the sensor to DMMP also in the presence of the common analytes in the air (24 000 ppm of water, 400 ppm of CO<sub>2</sub>, 5 ppm of NO, and 10 ppm of CO). We also tested the selectivity in competition with triethyl-phosphite (Et<sub>3</sub>P), phosphocholine (Pho-Ch, used as phosphocholine chloride calcium salt tetrahydrate simulant of V series), triphenylphosphine (PPh<sub>3</sub>) and methanol: in particular, we exposed BDPy-NH<sub>2</sub> to a large excess of these substances (50 equiv), and then 1 equivalent of DMMP was added. As shown in Figure 2, BDPy-NH<sub>2</sub> recognizes DMMP also in the presence of a large excess of the competitors. We note that BDPy-NH<sub>2</sub> recognizes phosphocholine with lower affinity respect to DMMP, suggesting a selectivity of the sensor for G series CWAs. Probably, the presence of the cationic aliphatic chain in the phosphocholine scaffold leads to a lower response of the probe.<sup>[32]</sup>

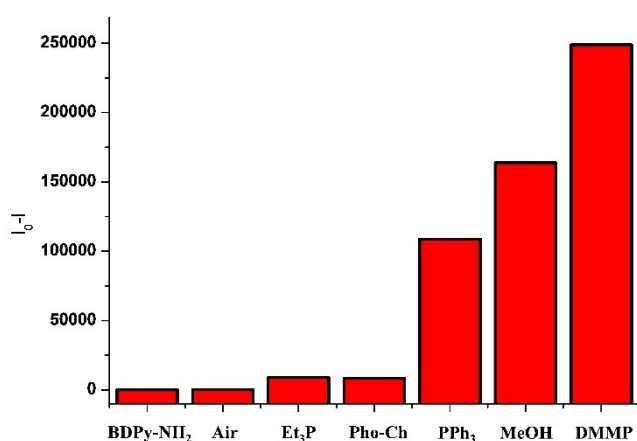
In order to obtain a real-world sensor device, we developed a prototypal solid-supported test strip. We tested the sensing properties of BDPy-NH<sub>2</sub> under realistic conditions: in air, by exposing to CWA vapors. Test strip was performed by dropping 2  $\mu$ L of the sensor solution (0.1 mM in CH<sub>2</sub>Cl<sub>2</sub>) onto neutral alumina substrate and exposing it to progressive amounts of DMMP vapors into a closed vial for 1 h at 50 °C. Although DMMP sensing by BDPy-NH<sub>2</sub> is instantaneous (as demonstrated by the measurements in solution), we attempted this time to lead the DMMP evaporation. Control tests were performed by spotting fluorescent carbon nanoparticles onto same strip and exposed it to the same amounts of the simulant.

Figure 3a shows the effect of the interaction of the sensitive probe as the amount of simulant increases. The image reveals an increase in fluorescence intensity as the analyte concentration rises. Thanks to the emission in the visible range when illuminated in the ultraviolet, it was possible to acquire images of the test strips by means of a standard smartphone. A simple image processing allowed us to perform a cross section analysis of the pixel intensity expressed in grayscale.

The figure shows that the control spots (on the left of each test strip) are not affected (constant fluorescence intensity) by increasing the concentration of nerve gas simulant, whereas the



**Figure 1.** Emission spectra of BDPy-NH<sub>2</sub> ( $1 \times 10^{-6}$  M in CHCl<sub>3</sub>,  $\lambda_{\text{ex}} = 500$  nm) upon the addition of DMMP. Inset: intensity changes upon the progressive addition of DMMP equivalents.



**Figure 2.** Normalized fluorescence responses of BDPy-NH<sub>2</sub> ( $1 \times 10^{-6}$  M in CHCl<sub>3</sub>,  $\lambda_{\text{ex}} = 500$  nm) to air (bubbled for 5 min), other competitive guests (50 equiv of triethyl-phosphite, phosphocholine, triphenylphosphine and methanol), and DMMP (1 equiv). Bars represent the initial over the final emission intensity at 530 nm.

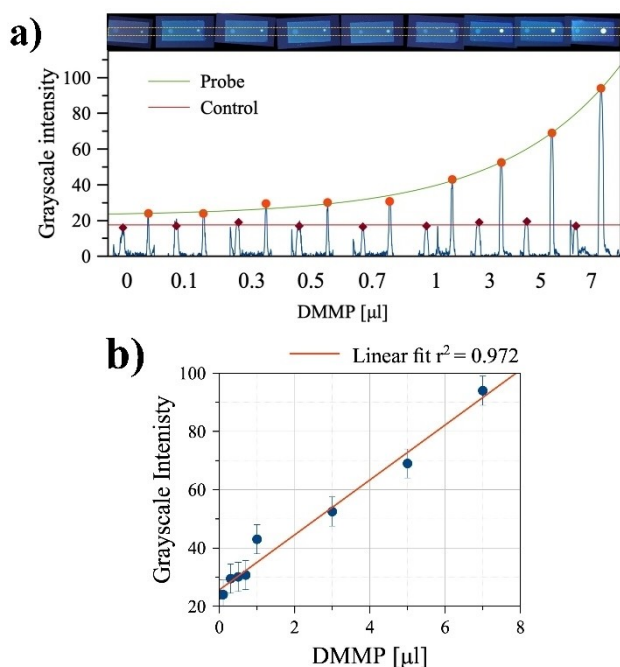


**Figure 3.** a) Photos of test strips and relative grayscale intensities. b) Correlation between the concentration of DMMP and the fluorescence intensity of the BDPy-NH<sub>2</sub> probe.

spot value relative to BDPy-NH<sub>2</sub> increases. Moreover, Figure 3b shows that there is a very good linear correlation between the concentration of the analyte and the fluorescence intensity of the probe.

Due to the similar volatility value of DMMP (5562 mg/m<sup>3</sup> at 25 °C) with respect to the G-type CWAs, this test strip may also be validated for real nerve agents. Furthermore, the LC<sub>50</sub> (concentration–time product, that is, lethal to 50% of those exposed and reflects toxicity by the inhalational route) of G-type CWAs are in the range 1.5–24 ppm × m<sup>3</sup> × h<sup>-1</sup>, thus this prototype can reveal CWAs under the lethal dose.

Recovery of the starting device was performed exposing the sensor to acidic water solution (pH 3) and then to alkaline water solution (pH 11; Figure 4a).<sup>[33]</sup> Low pH values lead to the protonation of nitrogen atoms, thereby breaking the supramolecular complex with DMMP.

Then, the starting sensor can be restored by the addition of a base. Image processing of the fluorescence spot intensity confirms the recovery of the initial luminescence (Figure 4a). We again exposed the device to DMMP for several cycles, thereby demonstrating that the sensing ability is maintained for at least 5 cycles (Figure 4c, more cycles have been precluded due to the destruction of the neutral alumina support).

In conclusion, a new fluorescent sensor able to interact noncovalently with DMMP has been synthesized and tested both in solution and in the gas phase. The detection limit in solution is about 10 ppt, much lower than the toxicity values of CWAs. In addition, CWA sensing in the gas phase can be performed by using a simple smartphone. With acid/base treatment, the solid device can be reused almost 5 times. We

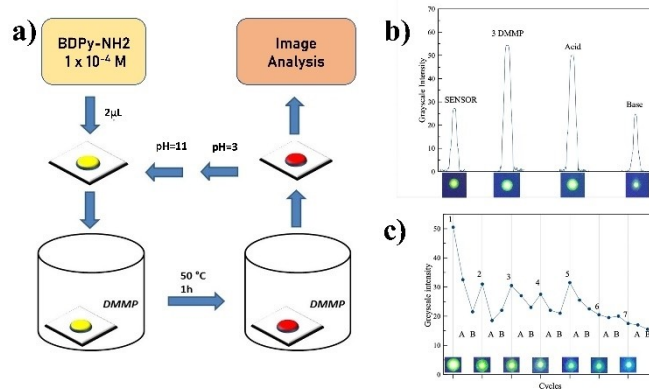


**Figure 4.** a) Schematic representation of gas-phase sensing by using a test strip and recovery of the sensor. b) Image analysis of the device during recovery. c) Image analysis during the recovery cycles.

are currently working on optimizing the solid support in order to increase the robustness of the device towards the acid/base cycles, thus improving the recovery properties. In addition, we are working on the functionalization of the sensor to improve the selectivity towards compounds with a P=O group. This prototype paves the way for the smart detection of nerve agents.

## Acknowledgements

This research was funded by the University of Catania for financial support. G. T. S. acknowledges the University of Catania for the funding received under the starting grant “DetCWAs” (PIA.CE.RI 2020-2022-Linea Intervento 3). N. T. thanks the Nai4Smart Project of the “Programma di ricerca di Ateneo UNICT 2020-22 Linea 2” for partial funding. A. P. acknowledges funding received on this project from Università degli Studi di Catania under the grant scheme PIACERI with the project MAF-moF “Materiali multifunzionali per dispositivi micro-optofluidici”. Open Access Funding provided by Università degli Studi di Catania within the CRUI-CARE Agreement.

## Conflict of Interest

The authors declare no conflict of interest.

**Keywords:** CWAs · fluorescent · sensing · supramolecular · smartphone

- [1] G. Mercey, T. Verdelet, J. Renou, M. Kliachina, R. Baati, F. Nachon, L. Jean, P.-Y. Renard, *Acc. Chem. Res.* **2012**, *45*, 756–766.
- [2] A. Zammataro, R. Santonocito, A. Pappalardo, G. Trusso Sfrassetto, *Catalysts* **2020**, *10*, 881.
- [3] German Federal Government, Statement by the Federal Government on the Navalny case, <https://www.bundesregierung.de/breg-en/news-statement-by-the-federal-government-on-the-navalny-case-1781882>.
- [4] R. Stone, *Science* **2018**, *359*, 1314–1315.

- [5] T. Nakagawa, A. T. Tu, *Forensic Toxicol.* **2018**, *36*, 61–71.
- [6] K. Kupferschmidt, *Science* **2019**, *365*, 1362.
- [7] D. D. Haines, S. C. Fox, *Forensic Sci. Rev.* **2014**, *26*, 97–114.
- [8] S.-H. Park, N. Kwon, J.-H. Lee, J. Yoon, I. Shin, *Chem. Soc. Rev.* **2020**, *49*, 143–179.
- [9] Y. J. Jang, K. Kim, O. G. Tsay, D. A. Atwood, D. G. Churchill, *Chem. Rev.* **2015**, *115*, PR1–PR76.
- [10] M. R. Sambrook, S. Notman, *Chem. Soc. Rev.* **2013**, *42*, 9251–9267.
- [11] J. R. Hiscock, F. Piana, M. R. Sambrook, N. J. Wells, A. J. Clark, J. C. Vincent, N. Busschaert, R. C. D. Brown, P. A. Gale, *Chem. Commun.* **2013**, *49*, 9119–9121.
- [12] A. Barba-Bon, A. M. Costero, M. Parra, S. Gil, R. Martínez-Máñez, F. Sancenón, P. A. Gale, J. R. Hiscock, *Chem. Eur. J.* **2013**, *19*, 1586–1590.
- [13] S. Chen, Y. Ruan, J. D. Brown, J. Gallucci, V. Maslak, C. M. Hadad, J. D. Badjić, *J. Am. Chem. Soc.* **2013**, *135*, 14964–14967.
- [14] Y. Ruan, E. Dalkılıç, P. W. Peterson, A. Pandit, A. Dastan, J. D. Brown, S. M. Polen, C. M. Hadad, J. D. Badjić, *Chem. Eur. J.* **2014**, *20*, 4251–4256.
- [15] S. Chen, Y. Ruan, J. D. Brown, C. M. Hadad, J. D. Badjić, *J. Am. Chem. Soc.* **2014**, *136*, 17337–17342.
- [16] Y. Ruan, S. Chen, J. D. Brown, C. M. Hadad, J. D. Badjić, *Org. Lett.* **2015**, *17*, 852–855.
- [17] A. Gulino, G. Trusso Sfrazzetto, S. Millesi, A. Pappalardo, G. A. Tomaselli, F. P. Ballistreri, R. M. Toscano, L. Fragalà, *Chem. Eur. J.* **2017**, *23*, 1576–1583.
- [18] R. Puglisi, P. G. Mineo, A. Pappalardo, A. Gulino, G. Trusso Sfrazzetto, *Molecules* **2019**, *24*, 2160.
- [19] R. Puglisi, A. Pappalardo, A. Gulino, G. Trusso Sfrazzetto, *Chem. Commun.* **2018**, *54*, 11156–11159.
- [20] R. Puglisi, A. Pappalardo, A. Gulino, G. Trusso Sfrazzetto, *ACS Omega* **2019**, *4*, 7550–7555.
- [21] L. Legnani, R. Puglisi, A. Pappalardo, M. A. Chiacchio, G. Trusso Sfrazzetto, *Chem. Commun.* **2020**, *56*, 539–542.
- [22] N. Tuccitto, L. Riela, A. Zammataro, L. Spitaleri, G. Li Destri, G. Sfuncia, G. Nicotra, A. Pappalardo, G. Capizzi, G. Trusso Sfrazzetto, *ACS Appl. Nano Mater.* **2020**, *3*, 8182–8191.
- [23] N. Tuccitto, L. Spitaleri, G. Li Destri, A. Pappalardo, A. Gulino, G. Trusso Sfrazzetto, *Molecules* **2020**, *25*, 5731.
- [24] C. M. A. Gangemi, U. Rimkaite, A. Pappalardo, G. Trusso Sfrazzetto, *RSC Adv.* **2021**, *11*, 13047–13050.
- [25] A. Pappalardo, C. M. A. Gangemi, R. M. Toscano, G. Trusso Sfrazzetto, *Curr. Org. Chem.* **2020**, *24*, 2378–2382.
- [26] J. Lavoie, S. Srinivasan, R. Nagarajan, *J. Hazard. Mater.* **2011**, *194*, 85–91.
- [27] R. J. Ellaby, E. R. Clark, N. Allen, F. R. Taylor, K. K. L. Ng, M. Dimitrovski, D. F. Chu, D. P. Mulvihill, J. R. Hiscock, *Org. Biomol. Chem.* **2021**, *19*, 2008–2014.
- [28] Y. Gabe, Y. Urano, K. Kikuchi, H. Kojima, T. Nagano, *J. Am. Chem. Soc.* **2004**, *126*, 3357–3367.
- [29] R. Ziessel, L. Bonardia, G. Ulrich, *Dalton. Trans.* **2006**, *35*, 2913–2918.
- [30] J. Zhang, N. Wang, X. Ji, Y. Tao, J. Wang, W. Zhao, *Chem. Eur. J.* **2020**, *26*, 4172–4192.
- [31] E. Butera, A. Zammataro, A. Pappalardo, G. Trusso Sfrazzetto, *ChemPlusChem* **2021**, *86*, 681–695.
- [32] Scarce selectivity results were obtained when using acetone, probably due to the interaction of the solvent with the probe. Organic acids were also tested; however, the protonation of the nitrogen atoms of the probe leads to quenching of the emission.
- [33] A recovery test with other organic solvents was precluded by the interaction of the sensor dropped onto the surface with the solvent, which leads to migration on the surface.

Manuscript received: June 13, 2021  
Version of record online: August 20, 2021